



Tailor-made gold nanostar colorimetric detection determined by morphology change and used as an indirect approach by using hydrogen peroxide to determine glucose concentration



Danielle Wingrove Mulder*, Masauso Moses Phiri, Barend Christiaan Vorster

Center for Human Metabolomics, North-West University, Hoffman street, Potchefstroom, South Africa

ARTICLE INFO

Keywords:

Biosensor
Gold nanostars
HEPES
Hydroxylamine hydrochloride
Hydrogen peroxide
Sodium hydroxide

ABSTRACT

Gold nanostars are being utilized more regularly in the field of nanodiagnostics. The modified seedless synthetic method comprised of 4-(2-hydroxyethyl)-1-piperazineethanesulfonic acid (HEPES) synthesized with the addition of silver nitrate was applied for a biosensor application. The colorimetric ability of these newly synthesized nanostars showed to be more sensitive and more visually colorful than the HEPES gold nanostars synthesized without silver nitrate. It was observed that the gold nanostar colorimetric assay could be tailored for a specific application using either hydroxylamine or sodium hydroxide as colorimetric catalysts. Upon the attachment of glucose oxidase to the gold nanostars, glucose was measured by its oxidation and the generated hydrogen peroxide resulted in a sufficient color gradient that clearly distinguished different concentrations. Added to the color changes was the spectrophotometric localized surface plasmon resonance peak shifts in response to different glucose concentrations. In conclusion, the reported nanostars showed great potential as a good biosensing candidate.

1. Introduction

Gold (Au) nanoparticles are ultrafine particles which are being used diversely in the medical field in areas such as immunosensing, biolabels and drug delivery [1,2]. This has proven valuable in disease diagnosis, treatment and prevention [3]. What makes gold nanoparticles an attractive platform for biosensing is their facile synthesis; unique properties (especially the colorimetric and physical properties) which allow for easy manipulation and design; and easy surface functionalization with biorecognition molecules [4]. Functionalized gold nanoparticles have been successfully used for protein, enzyme, oligonucleotide, metal ions and small molecule detection and can act as both the molecular acceptor as well as the signal transducer enhancing the sensitivity of a sensor [5,6]. Anisotropic gold nanoparticles such as gold nanostars are a promising alternative for biosensor application as the protruding arms add to the plasmonic contributions and the lightning rod effect. The surface plasmon resonance of the gold nanostars can be altered by controlling the gold nanostar arm density and length while maintaining the dimensional aspects [2].

Various synthesis methods for gold nanostars have been proposed. Of note are the seeded and seedless methods. The seedless method has been observed to be simpler in that it requires fewer steps and reagents.

2-[4-(2-hydroxyethyl)piperazinyl]ethanesulfonic acid (HEPES) has been used for the synthesis of gold nanostars as a green synthesis. The piperazine in the buffer generates nitrogen-centered free radicals which is responsible for reducing the gold ions (AuCl_4^-). The buffer acts as the growth-directing, reducing and capping agent for the nanostars [6–8]. Silver nitrate was added in a recent modified synthesis method for gold nanostars to overcome the dimensional control challenge pertaining to gold nanostars synthesized with the seedless method [9]. The added silver nitrate is reported to have had a shape-directing influence in the seedless method resulting in more monodispersed and multi-branched morphologies of gold nanostars [10,11].

Gold nanostars have been used as detectors for hydrogen peroxide sensing via the biocatalytic growth of the nanoparticles [12,13]. In an earlier publication it was shown that due to a biorecognition event which generated a hydrogen peroxide by-product, silver ions were reduced around the gold nanostar nanosensors which resulted in a localized surface plasmon resonance (LSPR) shift [3]. This shift is due to a change in the surface electron oscillations which may be influenced by shape, size, dielectric environment, surface coating and nanoparticle-chemical entity interaction, and can be detected by changes in scattering or absorption spectra or color variation of the nanoparticle solution [14]. Changes in essential parameters such as pH, and others, can

* Corresponding author.

E-mail address: 26718944@g.nwu.ac.za (D. Mulder).

<https://doi.org/10.1016/j.sbsr.2019.100296>

Received 8 April 2019; Received in revised form 31 July 2019; Accepted 6 August 2019

2214-1804/ © 2019 The Authors. Published by Elsevier B.V. This is an open access article under the CC BY-NC-ND license (<http://creativecommons.org/licenses/by-nc-nd/4.0/>).

exert a huge impact on the size, morphology, crystallinity and degree of aggregation of the nanostars thereby altering or modifying the response of the signal generation [12]. To this end various bases have been reported to catalyze the tunability of the morphology of the gold nanostars by the coating of silver or gold chloride ions [4,12,14–16].

Enzymes, such as glucose oxidase (GOx); which has been used extensively as a model enzyme in various fields, including nanotechnology biosensor applications, have been used to grow nanoparticles for optical detection applications [7,13,15]. GOx is a typical dimeric flavin enzyme with a molecular weight of approximately 150 kDa. It also contains 1 flavin adenine dinucleotide (FAD) cofactor per monomer. The main biological function of glucose oxidase is to catalyze the oxidation of β -D-glucose producing β -D-glucono-1,5-lactone and hydrogen peroxide [8,17]. The analytical range for glucose concentration used in current laboratory diagnostic tests in plasma ranges from 3 mmol/L–16.5 mmol/L [9,11]. The presence of hydrogen peroxide is used as an indirect approach to determining the glucose concentration [10]. Wilner's group showed that by using the oxidation of glucose by glucose oxidase, the hydrogen peroxide by product was able to act as a reducing agent for the deposition of gold onto gold nanoparticle surfaces [13].

Here we investigated the biosensing potential of our previously reported silver assisted seedless nanoparticle synthesis method compared to the HEPES only method. The effect of using both a weak and a strong base catalyst in the colorimetric reaction was also assessed. Additionally we assessed if this system could still produce a color change once functionalized with with GOx as a model enzyme.

2. Materials and method

2.1. Materials

4-(2-hydroxyethyl)-1-piperazineethanesulfonic acid (HEPES), gold (III) chloride trihydrate, silver nitrate, polyvinylpyrrolidone (PVP) 10,000, sodium hydroxide, hydroxylamine hydrochloride, 3,3'-dithiobis (sulfosuccinimidyl propionate) (DTSSP), glucose oxidase from *Aspergillus niger* (GOx) were purchased from Sigma-Aldrich. Glucose was from Dis-Chem pharmacy, South Africa. The nanostars were prepared in 5 mL screw cap tubes (Ascendis Medical) and all assays were carried out in 96-well plates (Corning).

2.2. Preparation of gold nanostars

Gold nanostars by a HEPES only method (Au⁻) were synthesized according to Xie et.al [18]. Briefly, 3 mL deionized water (Millipore, 18.2 Ω M) was added to 2 mL 100 mM HEPES buffer (pH 7.4), followed by the addition of 20 μ L of a 50 mM gold (III) chloride trihydrate aqueous solution. After gentle mixing the solution was left to stand at room temperature until the solution turned a greenish blue color.

Silver assisted gold nanostars (Au⁺) were synthesized as previously described by our group [19]. Briefly, deionized water (Millipore, 18.2 Ω M) was added to 100 mM HEPES buffer (pH 7.4), followed by the sequential addition of 20 μ L of a 50 mM gold (III) chloride trihydrate and 4 μ L of a 1 mM silver nitrate solution. The solution was mixed by end-to-end tube inversion and left to stand at room temperature for approximately 30 min until the solution turned a blue color. In both instances the nanostars were PVP coated. To each solution of nanostars 25 mM PVP was added after which the tubes were inverted a few times and left to stand at room temperature overnight. The samples were then centrifuged and resuspended in 500 μ L deionized water.

2.3. Glucose oxidase functionalized nanostars (Au-GOx)

2 mL of previously prepared Au⁺ gold nanostars coated with 2.5 mM PVP resuspended in 100 mM HEPES pH 6.9 was incubated with 100 μ L 0.5 mM DTSSP for 3 h at room temperature. Following this

150 μ L 2 mg/mL GOx was added to the tubes. The solution was then left in the fridge overnight for attachment of the GOx to the nanostars. Excess DTSSP and GOx was removed by several cycles of centrifugation at 2110 \times g for 50 min and resuspended with deionized water. This concentration of GOx was chosen as there was no aggregation of the nanostars during the clean-up process.

2.4. Colorimetric assays

Reagents were added and pipette mixed in the following order: 1 mM MES buffer pH 6, 15 μ L nanostars, 0–3 mM range hydrogen peroxide, 0.1 mM silver nitrate and 0.25 mM hydroxylamine hydrochloride. As an initial step a volume of deionized water was added that ensured a final volume of 200 μ L and reagent concentrations as stated above. A multi-channel pipette was used for adding the hydroxylamine hydrochloride. The samples were left to stand at room temperature for 60 min and then read on the microplate reader (400–900 nm). The same procedure was followed for the sodium hydroxide, with the modification of decreasing the hydrogen peroxide molarity range to 0–0.03 mM and replacing the hydroxylamine hydrochloride with 5 mM sodium hydroxide. In addition the reagents were incubated for 5 min only prior to spectrophotometric measurement. Multiple titration assays were set-up where nanostar volume, buffer, hydrogen peroxide, silver nitrate and base concentrations were varied (results not shown). These were the hydrogen peroxide concentration ranges obtained where there were colorimetric and spectrophotometric differences across the range. The procedure for the Au-GOx nanostars was according to the sodium hydroxide procedure but incubation of the nanostars at 37 $^{\circ}$ C for 1 h with range 0–0.015 mM glucose prior to a second 1 min incubation with silver and 4 mM NaOH gave optimal surface plasmon resonance properties.

2.5. Instrumentation

Characterization of nanostars was done with high resolution transmission electron microscopy (HR-TEM) and energy-dispersive spectroscopy (EDS), dynamic light scattering (DLS), nuclear magnetic resonance spectroscopy (NMR), agarose gel electrophoresis and ultraviolet visible spectroscopy (UV-Vis).

2.5.1. Morphology and elemental composition

The morphology and elemental composition of the nanostars were determined with HR-TEM and EDS on a JEOL JEM 2100F transmission electron microscope with Oxford instruments INCA 4.11 software as the corresponding EDS analysis software. Sample preparation was done by spotting the nanostars on to a copper grid and allowing them to air dry. DLS was used to estimate the hydrodynamic diameter of the PVP capped and Au-GOx nanostars. The analysis was performed on a Zetasizer Nano (Malvern) with the backscatter setting using Zetasizer version 6.20 software. The polystyrene cuvettes were stoppered to limit dust contamination.

2.5.2. Spectral properties

The absorbance spectrum of the nanostars was determined using a HT Synergy (BioTEK) microplate spectrophotometer operated between 400 and 800 nm at a 1 nm increment linked with the Gen5.1 analysis software.

2.5.3. Surface functionalization and charge

Successful enzyme attachment of GOx to Au⁺ nanostars was illustrated by comparison of NMR spectra, DLS, UV-Vis and agarose gel electrophoresis migration of Au⁺ nanostars with and without GOx functionalization. The NMR was performed at 500 MHz on a Bruker Avance III HD NMR spectrometer equipped with a triple-resonance inverse (TXI) 1H (15 N, 13C) probe head. The electrophoresis was done using 0.75% agarose and 1 \times Tris-EDTA buffer (TAE buffer) at pH 8.

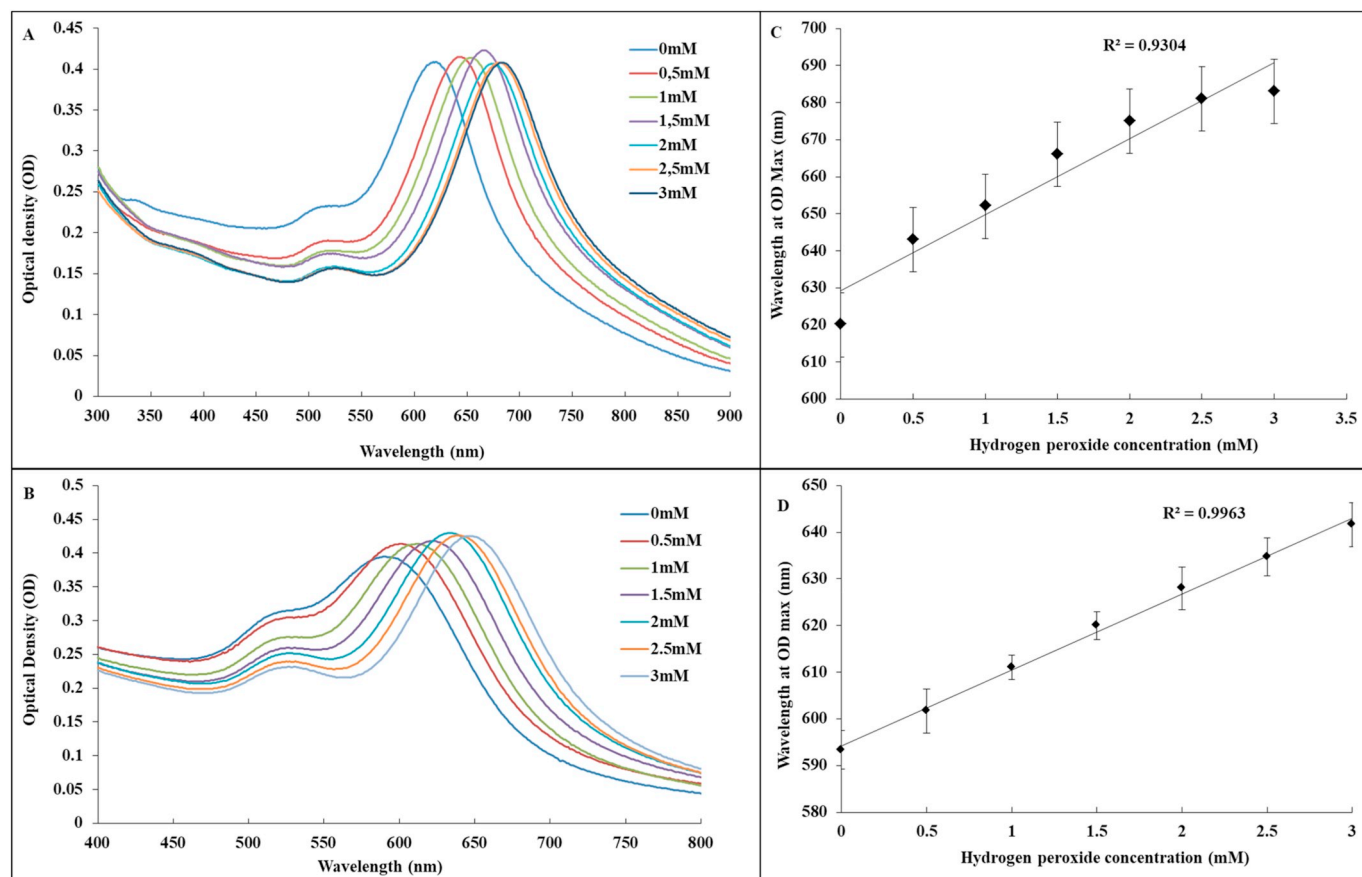


Fig. 1. Au⁻ and Au⁺ absorbance spectra and spectral shift linearity with hydroxylamine hydrochloride as the base. A) Au⁻ nanostars spectra. B) Au⁺ nanostars spectra. C) OD max of Au⁻ nanostars at varying hydrogen peroxide concentrations. D) OD max of Au⁺ nanostars at varying hydrogen peroxide concentrations.

The samples were prepared using 8 μ L nanostars mixed with 4 μ L 80% glucose and run at 40 V for approximately 45 min [20].

3. Results

The colorimetric assay results of the Au⁻ and Au⁺ nanostars with hydroxylamine hydrochloride as the base are presented in Fig. 1. In both instances a red shift of similar magnitude results from increasing hydrogen peroxide concentrations with a subsequent positive correlation between the observed OD max and concentration. The linear model fit and linear range of the Au⁺ nanostars were superior to that of the Au⁻ nanostars over the tested hydrogen peroxide range as judged visually and by the coefficient of determination.

The color change observed before and after incubation is presented in Fig. 2 for both the hydroxylamine hydrochloride and sodium hydroxide bases. For the hydroxylamine hydrochloride base, a dramatic change to red was observed for the Au⁺ in the absence of hydrogen peroxide which gradually became purple and then blue at 3 mM. In contrast to this the Au⁻ nanostars turned turquoise after incubation with greater intensity observed at low hydrogen peroxide concentrations.

The HR-TEM observed changes in morphology of the post-incubated Au⁺ nanostars at various hydrogen peroxide concentrations is presented in Fig. 3. Observing the morphology of the hydroxylamine hydrochloride assay, at low concentrations the morphology changed to predominantly spherical particles while a tendency towards maintaining the star morphology was observed at higher concentrations. In all instances small spherical structures are observed in addition to the nanoparticles. On average samples contained 87% elemental gold (Au) and 13% silver (Ag) as measured by EDS. The small spherical structures

were 100% Ag in composition. The size of these silver nanoparticles were approximately 12 nm in the absence of hydrogen peroxide and change to 6 nm at 0.5 mM and 4 nm for the rest of the hydrogen peroxide concentrations tested.

Fig. 4 shows the UV-vis spectra obtained from the colorimetric assay of the Au⁻ and Au⁺ gold nanostars when sodium hydroxide is used as the base. The linear model fit of the Au⁺ nanostars is again superior to that of the Au⁻ nanostars but in this instance a blue shift results from increasing hydrogen peroxide concentrations with a subsequent negative correlation between the OD max and increasing concentration.

In similar fashion the visually observed color change, as presented in Fig. 2 is comparable to the results obtained for hydroxylamine hydrochloride with Au⁺ nanostars showing a superior range of color change when compared to Au⁻ albeit with the change in the opposite direction. As is to be expected by now the HR-TEM images of the Au⁺ nanostars in sodium hydroxide, where to a large extent the opposite image of the same nanostars incubated with hydroxylamine hydrochloride, presented in Fig. 3. Nanostars at 0 mM and 0.005 mM hydrogen peroxide concentrations remained predominantly star shaped with a tendency to become spherical as the concentration increased to 0.03 mM. On average samples contained 77% Au and 23% Ag. Smaller 100% silver nanoparticles were again observed and measured approximately 2 nm and 4 nm at 0 mM and 0.005–0.01 mM respectively and 8 nm in the remainder of the samples.

Following these initial observations the Au⁺ nanostars were selected for functionalization with glucose oxidase. Evidence of successful functionalization is presented in Fig. 5. When compared to Au⁺ nanostars, the NMR spectra of the Au-GOx nanostars shows loss of peaks associated with PVP capping and a prominent additional peak at

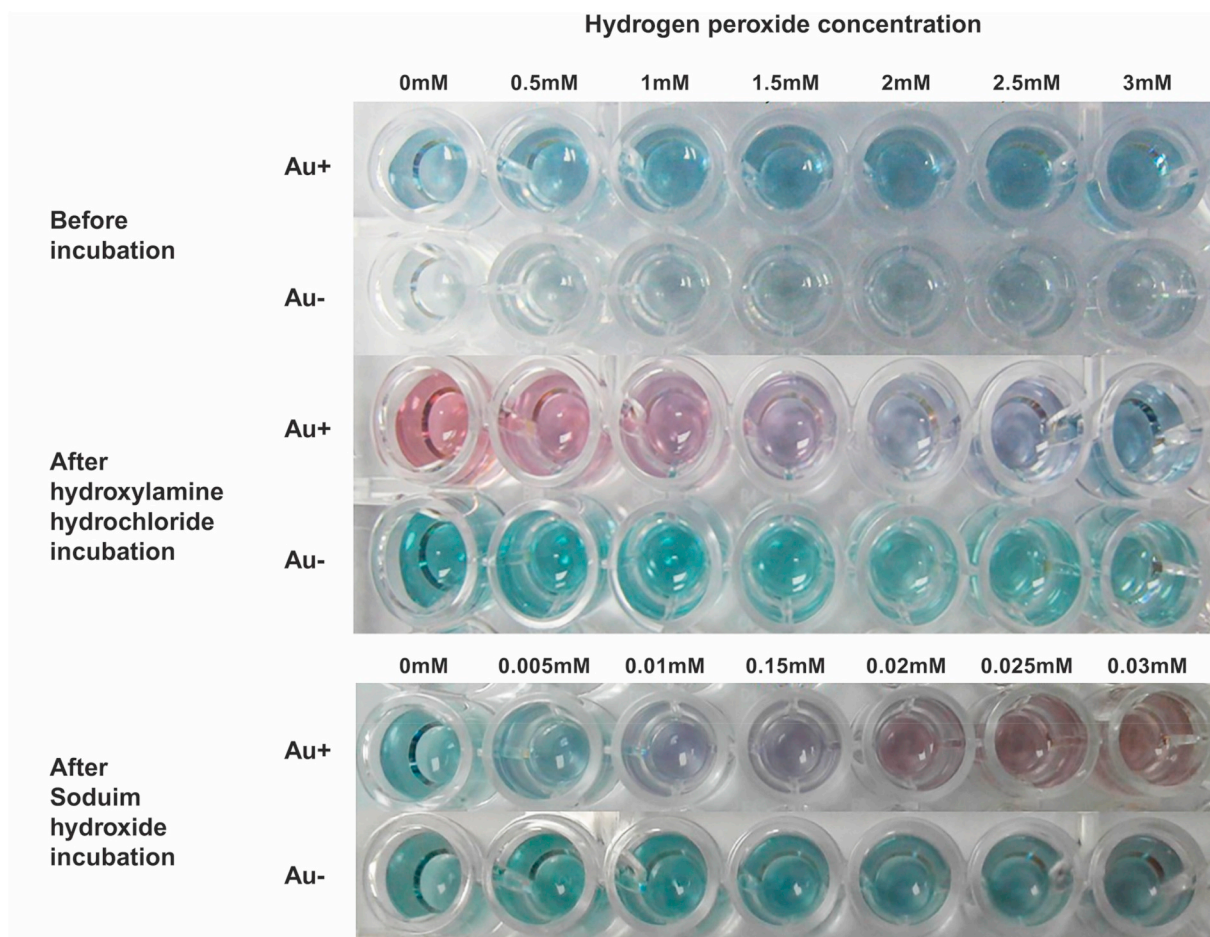


Fig. 2. Photograph of the Au+ and Au- nanostars colorimetric assay before incubation and after incubation for both hydroxylamine hydrochloride and sodium hydroxide with increasing hydrogen peroxide concentrations.

approximately 3.7 ppm due to attachment of GOx. Reference spectra for the various components have been published previously [19,21]. When compared to Au+ nanostars, the Au-GOx nanostars migrated cathodally to a lesser extent indicating an increase in size and/or a decrease in net negative charge. Some broadening of the bands are also observed with greater prominence of the application site. This is likely due to an increased tendency towards aggregation due to loss of PVP coating. The hydrodynamic diameter increased from approximately 49 nm to 62 nm when the Au+ nanostars were compared to the Au-GOx nanostars on DLS with similar polydispersity indices (0.39 and 0.32 respectively) while the OD max of the UV-vis spectra showed a red shift from 688 nm to 711 nm with broadening of the peak. The presence of the enzyme would result in a larger hydrodynamic diameter [19,20] and was found to increase from 49.27 nm to 62.00 nm.

A pilot study for the colorimetric assay for the Au-GOx nanostars using sodium hydroxide as the base is presented in Fig. 6. It has been shown that gold nanoparticles can oxidize glucose generating hydrogen peroxide and gluconic acid [22], however, no changes in color was observed when various components of the reaction mixture was omitted (Fig. 6). In agreement with the previous finding when sodium hydroxide was used as a base, an increase in the blue shift of the OD max was observed with increasing hydrogen peroxide concentrations with good linearity and model fit over the tested range (Fig. 7). The corresponding visual color change is presented in Fig. 8 which largely shows a blue to green change in color with concomitant increase with increasing glucose concentrations.

4. Discussion

We have shown previously that the Au+ had a structural advantage over the Au- nanostars, however, there was need to examine if these structural advantages translated into additional benefit for potential analytical applications. Generally, the Au+ nanostars outperformed the Au- ones in terms of the analytical range of the absorbance shift and its associated visual observability. The two different bases i.e. hydroxylamine hydrochloride and sodium hydroxide, also had varying results in the colorimetric sensing based on hydrogen peroxide reduction of silver onto the gold nanostars. Ammonia was also tried as a catalyst as used by Rodríguez-Lorenzo et al. [12], however, no color change was observed with the nanostars.

The data obtained by using hydroxylamine hydrochloride as the base showed a red shift for both the Au+ and Au- spectra. The shift of the Au+ nanostars showed a better linearity compared to the Au- nanostars which was noted by the regression of the scatter plots allowing for hydrogen peroxide concentration determination. There was also an inverse relationship between maximum absorbance shift and concentration. The confluence of the Au+ spectra was more pronounced than that observed by the Au- nanostars suggesting the shortening of the Au+ nanostar branches in the absence of hydrogen peroxide and a maintenance of the arm integrity in the presence of increased hydrogen peroxide concentration. This is seen by the lessening of the shoulder peak while maintaining the main peak [19]. The color change was attributed to the change in morphology of the Au+ nanostars as seen with corresponding TEM images. In the absence of hydrogen peroxide, the nanostars changed shape to spherical with a

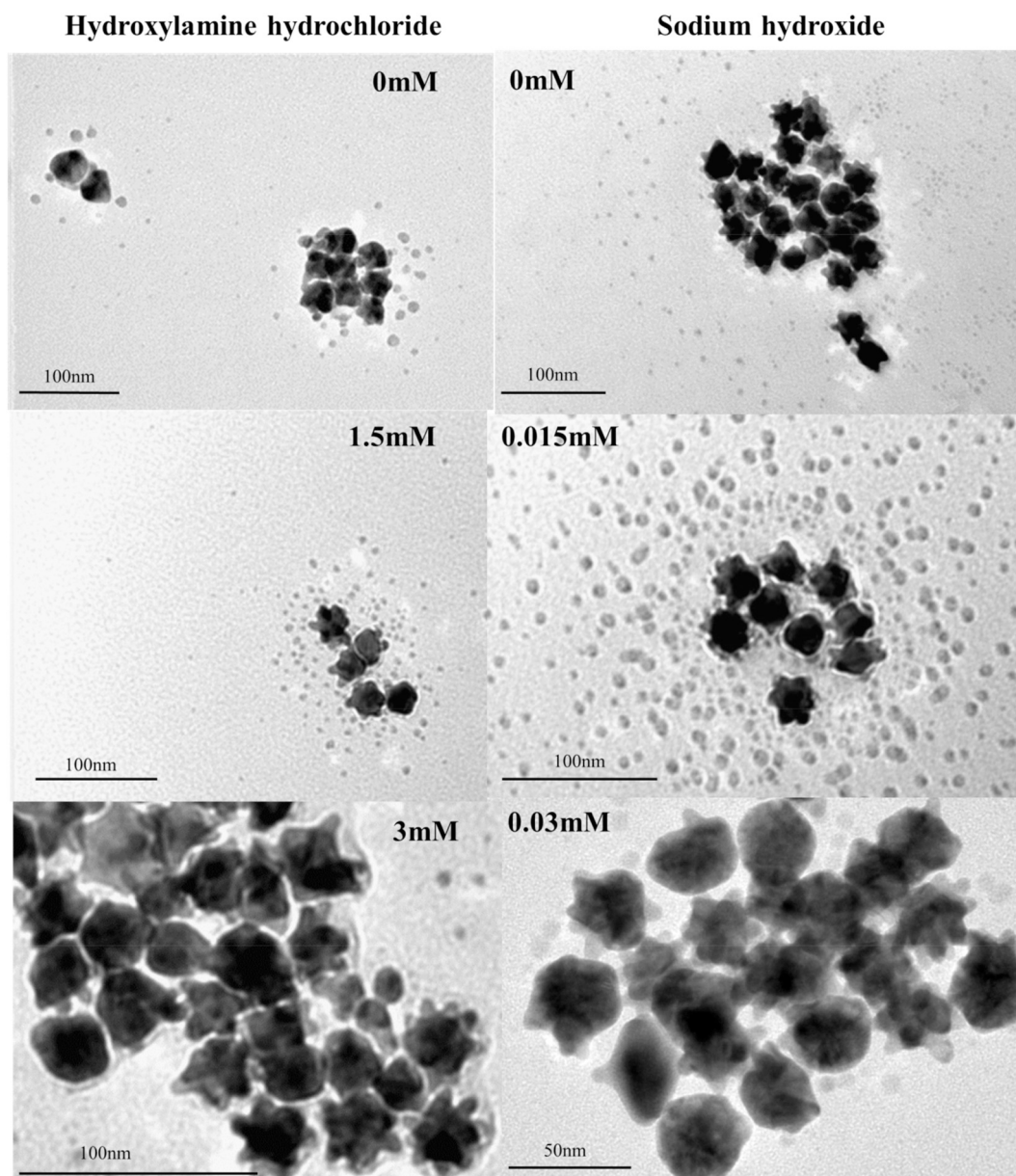


Fig. 3. TEM images of the post-incubation Au+ nanostars for both hydroxylamine hydrochloride and sodium hydroxide bases.

corresponding color change to red while the presence of hydrogen peroxide prevented this. Although the mechanism for this observation is yet to be elucidated, the empirical findings suggest that this assay may be particularly suited to the detection of absence of the target analyte.

In contrast, when sodium hydroxide was used as a base, a direct relationship was observed between maximum absorbance shift and concentration. In this reaction a distinct blue shift was obtained for the Au+ nanostars whereas the Au- nanostars had a marginal blue shift. The Au+ spectra became more confluent with increased hydrogen peroxide resulting in the highest concentration having an optical density maximum at 526 nm which is characteristic of spherical gold nanoparticles [23]. The TEM image obtained for this colorimetric range showed that the particles did become more spherical with the increase of hydrogen peroxide. This is a result of the hydrogen peroxide etching the gold nanostar into a spherical shape [24]. The distance of the various OD max for the Au+ nanostars and the intensity of the color change make this assay combination suitable for concentration determination assays. Although the incubation time for the sodium

hydroxide assay was only 5 min and substantially shorter than the 60 min required for the hydroxylamine hydrochloride assay, it should be noted that this parameter was not optimized exhaustively and further improvement of the reaction times of both assays may well be possible.

The optimal base for concentration determination was applied to a glucose assay. The intention of the glucose assay was to determine if the gold nanostar would continue to generate a color change if the hydrogen peroxide was generated by an enzyme-substrate reaction. Glucose oxidase was attached to the surface of the gold nanostar as it has been reported in literature that the stability of gold nanoparticles is increased with the functionalization of enzymes as well as improving enzyme performance [25,26]. This was also done considering the downstream application where the nanostars would be used in a more complex matrix such as plasma. Although the color change of the glucose was different from both the hydroxylamine hydrochloride and sodium hydroxide, as the color change was different shades of green, there was a sufficient shift in the spectra to determine the hydrogen peroxide concentration. In comparison to the glucose concentration

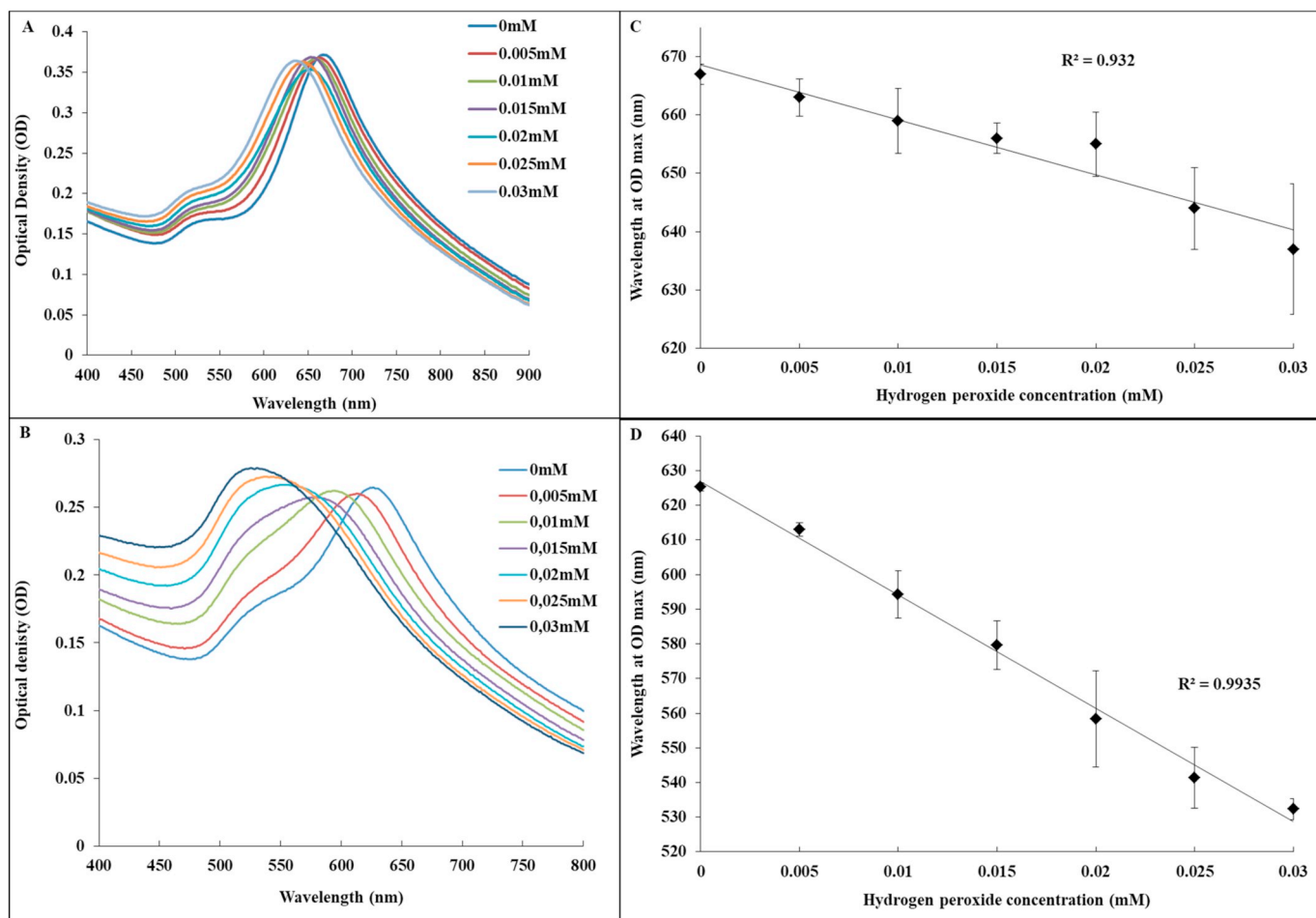


Fig. 4. Au⁻ and Au⁺ absorbance spectra and spectral shift linearity with sodium hydroxide as the base. A) Au⁻ nanostars spectra. B) Au⁺ nanostars spectra. C) OD max of Au⁻ nanostars at varying hydrogen peroxide concentrations. D) OD max of Au⁺ nanostars at varying hydrogen peroxide concentrations.

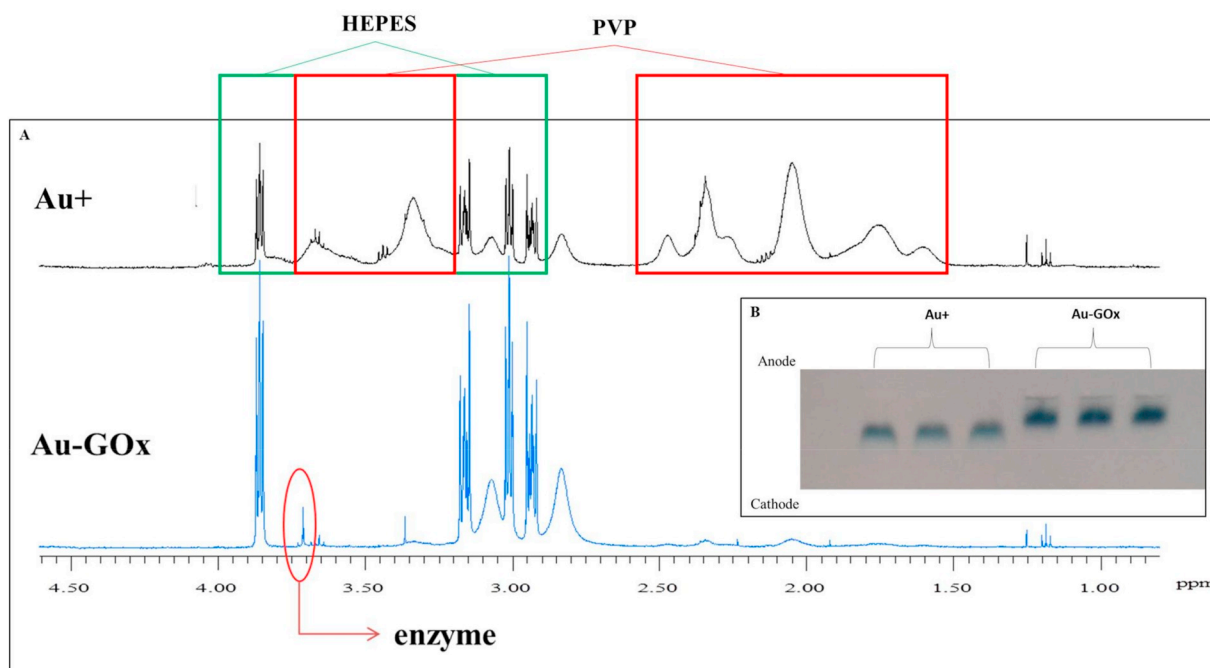


Fig. 5. A) NMR spectra and B) agarose gel electrophoresis of Au⁺ and Au-GOx nanostars suggesting successful functionalization.

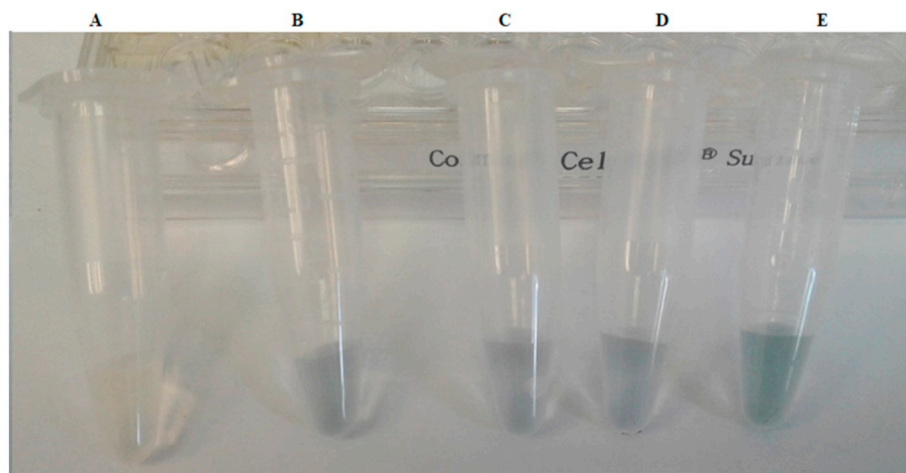


Fig. 6. Tubes containing all the reaction components with the following components omitted A) Au-GOx, B) glucose, C) silver nitrate, D) sodium hydroxide and E) all components present.

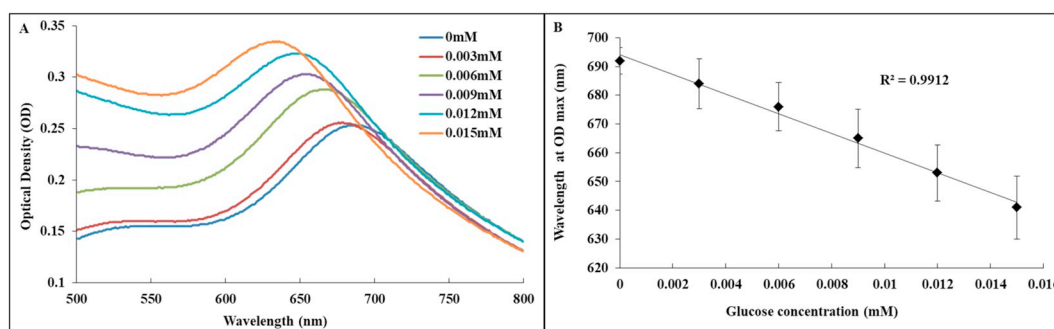


Fig. 7. A) Au-GOx absorbance spectra and B) spectral shift linearity at various glucose concentrations with sodium hydroxide as the base.

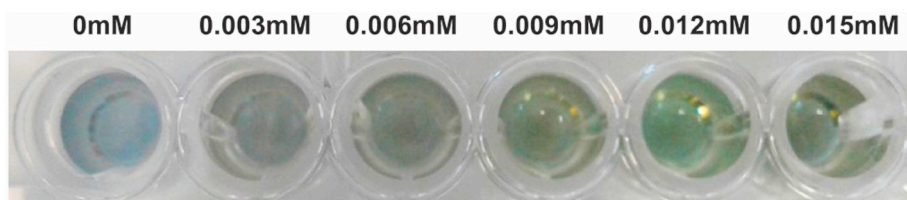


Fig. 8. Photograph of the Au-GOx colorimetric assay with sodium hydroxide as the base.

range currently detected in laboratories, the hydroxylamine hydrochloride assay was detecting a linearity between 0 mM – 3 mM hydrogen peroxide, the sodium hydroxide was 0 mM – 0.03 mM and the glucose oxidase assay was 0 mM - 0.015 mM. This observation renders the gold nanostar a sufficient platform for enzyme-substrate colorimetric assays.

5. Conclusion

The gold nanostars synthesized with the addition of silver nitrate showed to be more sensitive and reactive than the alternative HEPES synthesized nanostars. Depending on the desired application, the colorimetric assay can be tailor made. The hydroxylamine hydrochloride sample went from red to blue which would make it suitable in detecting the absence of an analyte, whereas, the sodium hydroxide was the reverse which makes it suitable for concentration dependent detection assays. Upon the introduction of the enzyme similar results were obtained which maintained the nanoparticle stability and a 0 mM – 0.015 mM sample range was needed for the system to function optimally. This biosensor combination holds promise as a new biosensor platform for enzyme-substrate colorimetric assays.

Funding

All authors were supported by the North-West University's Centre of Human Metabolomics (CHM) and the South African Technology Innovation Agency (TIA) to carry out this work.

Declaration of Competing Interest

The following authors have no financial disclosures, D.W.M, M.M.P and B.C.V.

Acknowledgements

We would like to acknowledge and thank Mrs. Erna Van Wilpe, Dr. Eudri Venter and Dr. Chantelle Venter at the Laboratory for Microscopy and Microanalysis at Pretoria University, South Africa for their time, advice and the use of their machine to obtain the EDS and TEM results for this article. We would also like to acknowledge and thank Dr. Shayne Mason from the Centre for Human Metabolomics, North-West University, Potchefstroom, South Africa for assistance with obtaining the NMR spectra.

References

- [1] H. Daraee, A. Eatemadi, E. Abbasi, S. Fekri Aval, M. Kouhi, A. Akbarzadeh, Application of gold nanoparticles in biomedical and drug delivery, *Artif. Cells Nanomed. Biotechnol.* 44 (1) (2016) 410–422.
- [2] A. Gerber, M. Bundschuh, D. Klingelhofer, D.A. Groneberg, Gold nanoparticles: recent aspects for human toxicology, *J. Occup. Med. Toxicol.* 8 (1) (2013) 32.
- [3] A.K. Khan, R. Rashid, G. Murtaza, A. Zahra, Gold nanoparticles: synthesis and applications in drug delivery, *Trop. J. Pharm. Res.* 13 (7) (2014) 1169.
- [4] Z. Liu, F. Zhao, S. Gao, J. Shao, H. Chang, The applications of gold nanoparticle-initiated chemiluminescence in biomedical detection, *Nanoscale Res. Lett.* 11 (1) (2016) 460.
- [5] G.A. Posthuma-Trumpie, J. Korf, A. van Amerongen, Lateral flow (immuno)assay: its strengths, weaknesses, opportunities and threats. A literature survey, *Anal. Bioanal. Chem.* 393 (2) (2009) 569–582.
- [6] K. Saha, S.S. Agasti, C. Kim, X. Li, V.M. Rotello, Gold nanoparticles in chemical and biological sensing, *Chem. Rev.* 112 (5) (2012) 2739–2779.
- [7] S.B. Bankar, M.V. Bule, R.S. Singhal, L. Ananthanarayan, Glucose oxidase — an overview, *Biotechnol. Adv.* 27 (4) (2009) 489–501.
- [8] S. Hu, Q. Lu, Y. Xu, CHAPTER 17 - biosensors based on direct electron transfer of protein, in: X. Zhang, H. Ju, J. Wang (Eds.), *Electrochemical Sensors, Biosensors and Their Biomedical Applications*. San Diego, Academic Press, 2008, pp. 531–581.
- [9] D.B. Sacks, D.E. Bruns, D.E. Goldstein, N.K. Maclaren, J.M. McDonald, M. Parrott, Guidelines and recommendations for laboratory analysis in the diagnosis and management of diabetes mellitus, *Clin. Chem.* 48 (3) (2002) 436–472.
- [10] T. Miyasaka, Y. Jinbo, K. Sakai, Y. Yoshimi, Determination of glucose concentration by electroluminescence of an indium-tin oxide electrode, *Food Bioprod. Process.* 76 (2) (1998) 102–106.
- [11] S.I. Sherwani, H.A. Khan, A. Ekhzaimy, A. Masood, M.K. Sakharkar, Significance of HbA1c test in diagnosis and prognosis of diabetic patients, *Biomark. Insights* 11 (2016) 95–104.
- [12] L. Rodríguez-Lorenzo, R. de la Rica, R.A. Álvarez-Puebla, L.M. Liz-Marzán, M.M. Stevens, Corrigendum: Plasmonic nanosensors with inverse sensitivity by means of enzyme-guided crystal growth, *Nat. Mater.* 17 (2) (2018) 204.
- [13] I. Willner, R. Baron, B. Willner, Growing metal nanoparticles by enzymes, *Adv. Mater.* 18 (9) (2006) 1109–1120.
- [14] L. Tang, J. Li, Plasmon-based colorimetric nanosensors for ultrasensitive molecular diagnostics, *ACS Sensors.* 2 (7) (2017) 857–875.
- [15] L. Liu, Y. Hao, D. Deng, N. Xia, Nanomaterials-based colorimetric immunoassays, *Nanomaterials.* 9 (3) (2019) 316.
- [16] C. Peng, X. Duan, G.W. Khamba, Z. Xie, Highly sensitive “signal on” plasmonic ELISA for small molecules by the naked eye, *Anal. Methods* 6 (24) (2014) 9616–9621.
- [17] S. Viswanathan, P. Li, W. Choi, S. Filipek, T.A. Balasubramaniam, V. Renugopalakrishnan, Chapter nine - protein-carbon nanotube sensors: single platform integrated micro clinical lab for monitoring blood analytes*, in: N. Düzgüneş (Ed.), *Methods in Enzymology*. 509, Academic Press, 2012, pp. 165–194.
- [18] J. Xie, J.Y. Lee, D.I.C. Wang, Seedless, surfactantless, high-yield synthesis of branched gold nanocrystals in HEPES buffer solution, *Chem. Mater.* 19 (11) (2007) 2823–2830.
- [19] D.W. Mulder, M.M. Phiri, B.C. Vorster, Modified HEPES one-pot synthetic strategy for gold nanostars. *Royal society open science*, Process 2019 (Submitted 30 Jan 2019), 2019.
- [20] H. de Puig, J.O. Tam, C.-W. Yen, L. Gehrke, K. Hamad-Schifferli, Extinction coefficient of gold nanostars, *J. Phys. Chem. C Nanomater. Interfaces* 119 (30) (2015) 17408–17415.
- [21] M.M. Phiri, D.W. Mulder, B.C. Vorster, Seedless gold nanostars with seed-like advantages for biosensing applications, *R. Soc. Open Sci.* 6 (2) (2019) 181971.
- [22] N.J. Lang, B. Liu, J. Liu, Characterization of glucose oxidation by gold nanoparticles using nanoceria, *J. Colloid Interface Sci.* 428 (2014) 78–83.
- [23] W. Haiss, N.T.K. Thanh, J. Aveyard, D.G. Fernig, Determination of size and concentration of gold nanoparticles from UV–Vis spectra, *Anal. Chem.* 79 (11) (2007) 4215–4221.
- [24] K. Nitinaivini, T. Parnklang, C. Thammacharoen, S. Ekgasit, K. Wongravee, Colorimetric determination of hydrogen peroxide by morphological decomposition of silver nanoprisms coupled with chromaticity analysis, *Anal. Methods* 6 (24) (2014) 9816–9824.
- [25] S. Ding, A.A. Cargill, I.L. Medintz, J.C. Claussen, Increasing the activity of immobilized enzymes with nanoparticle conjugation, *Curr. Opin. Biotechnol.* 34 (2015) 242–250.
- [26] J. Virkutyte, R.S. Varma, Green synthesis of metal nanoparticles: biodegradable polymers and enzymes in stabilization and surface functionalization, *Chem. Sci.* 2 (5) (2011) 837–846.



Danielle Wingrove Mulder is a registered medical scientist with a strong focus on research and development, especially that pertaining to human life improvement. She is currently a biochemistry Ph.D. candidate and employed as a research fellow with the Centre of Human Metabolomics at the North-West University (South Africa). She is busy designing a nanotechnological based assay for the detection of glycated haemoglobin and microalbumin used in Diabetes Mellitus. She also has a background in research and diagnostics in areas such as molecular biology, cellular biology, human genetics and wildlife forensics.



Masauso Moses Phiri is a Ph.D. Candidate with Biochemistry at the North-West University (South Africa). His main research focus is the development of nanotechnology-based biosensors for enzymatic assays. He holds a Bachelor's degree in Biomedical Sciences and two Master's degrees focused in Chemical Pathology and Biochemistry. He also works as a research fellow with the Centre for Human Metabolomics at the same university. His research interests are in the development of cost-effective methods for disease diagnosis for resource constrained regions.



Barend Christiaan Vorster is chemical pathologist and the director of the Centre for Human Metabolomics which was established as a joint venture between the North-West University and the Technology Innovation Agency of South Africa. He oversees several laboratories focused on metabolic diagnostics, newborn screening and metabolomics. His ambition is to provide diagnostic services for inherited metabolic and other diseases by translating sophisticated analytical infrastructure and methodologies into applications that is suited for Africa and South Africa in particular.